Journal of Alloys and Compounds 511 (2012) 123–128

Contents lists available at SciVerse ScienceDirect

Journal of Alloys and Compounds

journal homepage: www.elsevier.com/locate/jallcom

# Characterization and photoluminescent enhancement of $Li^+$ corporation effect on $CaWO_4:Eu^{3+}$ phosphor

Yeqing Chen [a], Hyun Kyoung Yang [a], Sung Wook Park [a], Byung Kee Moon [a], Byung Chun Choi [a], Jung Hyun Jeong [a,*], Kwang Ho Kim [b]

[a] Department of Physics, Pukyong National University, 599-4, Daeyeon 3-Dong, Nam-Gu, Busan 608-737, Republic of Korea
[b] School of Materials Science and Engineering, Pusan National University, Busan 609-735, Republic of Korea

ARTICLE INFO

*Article history:*
Received 12 July 2011
Received in revised form 5 September 2011
Accepted 5 September 2011
Available online 10 September 2011

*Keywords:*
Li-doping
Red phosphor
W-LED

ABSTRACT

The red-emitting phosphor of $Eu^{3+}$ ions doped $CaWO_4$ and lithium ions co-doped (Ca, Eu) $WO_4$ have been synthesized by the solid-state reaction technology. The introduction of $Li^+$ ions reduced the preparing temperature and the phosphors exhibited a very strong red emission. It is proved by X-ray diffraction and XPS spectrum that the $Li^+$ ion substituted the $Ca^{2+}$ in the lattice without changing the crystalline. The photoluminescence spectrum showed that after $Li^+$ doping, the dominant emission peak of $^5D_0$–$^7F_2$ centered at 617 nm was remarkably improved by a factor of 2.9, and the concentration quenching behavior was weakened until it is observed at 15 mol%. This is assigned to the incorporation of $Li^+$ into host twinning the $V''_{Ca}$ and making a Schottky pair for charge compensation. $Li^+$ acting as charge compensator is responsible for the enhancement of luminescent properties. The CIE coordinates were also calculated according to the NTSC system standard to be (0.682, 0.317), thus it is efficient enough to be used as red phosphor for NUV LED chips.



## 1. Introduction

Within the last several decades, much attention has been paid in replacing incandescent light sources by high-efficiency white light-emitting diodes (LED) [1,2]. As we all know, in a single white LED device, phosphor is one of the most indispensible materials in lighting technology, and thus it has been intensively investigated [3–6]. It is well known that a 450–470 nm blue-emitting diode excited yellow-emitting YAG:$Ce^{3+}$ phosphor has been widely used as the common white LED [7]. However, this kind of white light generated by blue chips with yellow phosphors has many disadvantages. The overall efficiency decreases rapidly if the correlated color temperature of the device is lowered. Besides, a lack of color rendering index (CRI) in output white light is urgent to be solved [8]. One of the resolutions to this problem is to use near UV LED chip excited RGB phosphors to obtain required color rendering properties.

Recently, the scheelite-structured orthotungstates and orthomolybdates with a general formula $ABO_4$ (A = Ca, Sr, Ba, Pb, Cd; B = W, Mo) have been extensively investigated owing to their wide potential industrial applications such as scintillators [9,10], phosphors [11,12], photocatalysts [13,14], batteries [15] and solid-state lasers [16,17]. Trivalent lanthanide ions, such as $Eu^{3+}$, provide quite a favorable situation for replacement in $A^{2+}$ sites with isostructural substitution. $Eu^{3+}$ ion taking a site without centro-symmetry enables the red emission from $^5D_0$–$^7F_2$ electric dipole transition, which is conducive to improving the color purity of the red phosphor. These $Eu^{3+}$ doped tungstate phosphors are relatively stable and have strong absorption in the near-UV region with good color purity, so they are promising candidates as red component for W-LEDs.

Most phosphors prepared by the conventional solid-state method require a relatively high temperature, which means a great amount of energy consumption in large scale production. Several investigations have been taken on the effect of $Li^+$ doping on luminescence properties. Recently, Bae et al. studied the enhancement of $Li^+$ doping on the luminescence property of $Y_2O_3:Eu^{3+}$ and $(Y,Gd)_2O_3$ [18,19]. Yeh and Su reported LiF doped into $Gd_2O_3$ as a lubricant, which increased the photoluminescence and thermoluminescence to a large amount by a complete incorporation of $Eu_2O_3$ into $Gd_2O_3$ lattice [20]. It was also reported by Byeon et al. that with addition of Li to $Gd_{1.8}Y_{0.2}O_3:Eu^{3+}$ greatly increased the PL intensity. Moreover, a slight red shift in charge transfer band (CTB) was also reported based on the results of XRD patterns and PL spectra [21]. However, few studies have investigated $Li^+$-doped $CaWO_4:Eu^{3+}$ phosphors with regard to luminescence consequently. In this paper, the $CaWO_4:Eu^{3+}$ and $Li^+$-doped $CaWO_4:Eu^{3+}$ phosphors were synthesized by solid-state reaction method. And the

* Corresponding author. Fax: +82 51 629 5549.
*E-mail address:* jhjeong@pknu.ac.kr (J.H. Jeong).

0925-8388/$ – see front matter © 2011 Elsevier B.V. All rights reserved.
doi:10.1016/j.jallcom.2011.09.004

enhanced luminescence properties and diminution of concentration quenching behavior were discussed.

## 2. Experiment

The $Ca_{1-x}Eu_xWO_4$ and $Ca_{1-2x}Eu_xLi_xWO_4$ ($x$ = 0.02–0.20 mol) phosphors were prepared by the solid-state reaction in air. A stoichiometric ratio of starting materials $CaCO_3$ (99.99%), $WO_3$ (99.9%), $Li_2CO_3$ (99.99%), and $Eu_2O_3$ (99.99%) were weighted and mixed in a planetary ball milling. It is reported that the particle size can be reduced to the 1–10 μm range by using planetary ball mill, which is very favorable to the sintering process in decreasing the temperature [24]. In order to prevent contamination and keep high purity, the high-rigidity ZrO balls were used. After 10 h of ball milling, the powder samples were calcined at 800, 900, 1000 and 1100 °C for 6 h in air. The structural characteristics and phase purity of the as-synthesized phosphors were measured by X-ray diffraction (XRD) patterns using a Philips, X'pert-MPD diffraction system, with Cu $K\alpha_1$ radiation λ = 1.54056 Å. The morphology and particle size of the final products were characterized with a field emission scanning electron microscope (SEM) (JEOL JSM-6700F) at 10 kV. The chemical states of the elements were analyzed by the X-ray photoelectron spectroscopy (XPS, ESCALAB 250, UK) with a monochromatic A1 Kα X-ray source ($h\nu$ = 1486.6 eV). C 1s at 284.6 eV served as the internal reference. The room temperature photoluminescence excitation (PLE) and PL spectra of the $Ca_{1-x}Eu_xWO_4$ and $Ca_{1-2x}Eu_xLi_xWO_4$ phosphors were recorded on PTI (Photon Technology International, USA) using a Xenon lamp with a power of 60 W. The lifetimes were measured using a phosphorimeter attachment to the main system with a Xe-flash lamp (25 W power) with a dominant excitation wavelength of 245 nm.

## 3. Results and discussion

### 3.1. Crystal structure and characterization

Fig. 1 shows the XRD patterns of $Ca_{0.9}Eu_{0.1}WO_4$, $Ca_{0.8}Eu_{0.1}Li_{0.1}WO_4$, no impurity peaks were observed, and all the reflection peaks could be well indexed to the JCPDS card of $CaWO_4$ No. 85-0443. Comparing these two kinds of samples prepared at 800–1000 °C, the position and intensity of the main peaks are approximately same with no shift or abatement. When the temperature is further increased to 1100 °C, the crystallinity is enhanced remarkably in the $Ca_{0.8}Eu_{0.1}Li_{0.1}WO_4$ XRD patterns, proved by the decreasing of the FWHM (full width at half-maximum) of the (1 1 2) peak from 0.116 to 0.083, as shown in the inset of Fig. 1b. The radius of $Eu^{3+}$ ion is known as 0.095 nm, which is similar to that of $Ca^{2+}$ (0.099 nm). Hence the $Eu^{3+}$ ion can successfully substitute $Ca^{2+}$ ion in $CaWO_4$ host lattice reflected by the diffraction patterns. It can be assumed that $Li^+$ ions do not occupy the space among the crystal lattice, but substitute the $Ca^{2+}$ ions and possess the site in the lattice. When the $CaWO_4$:$Eu^{3+}$ is obtained at 800 °C without $Li^+$ doping, the crystallinity is not so good as testified by relatively weak X-ray diffraction intensities. In contrast, the diffraction intensities of $Li^+$-doped $CaWO_4$:$Eu^{3+}$ are considerably increased due to much better crystallization even after sintering at the same temperature. The FWHM of the (1 1 2) peak of $Li^+$-doped $CaWO_4$:$Eu^{3+}$ is narrowed to a large extent from 0.142° to 0.083° in comparison of that of $CaWO_4$:$Eu^{3+}$. It is evidently demonstrated that the introduction of $Li^+$ ions plays the role of improving the crystallinity by incorporating $Eu_2O_3$ into $CaWO_4$ as well as $Li^+$ itself is incorporated into the host lattice during the sintering process.

### 3.2. Morphology and crystallization

The FE-SEM images of the $Ca_{0.9}Eu_{0.1}WO_4$ and $Ca_{0.8}Eu_{0.1}Li_{0.1}WO_4$ sintered at 800–1100 °C are compared in Fig. 2. It can be observed that the growth of $Ca_{0.9}Eu_{0.1}WO_4$ is not fully accomplished especially at low sintering temperature in Fig. 2(a) and (b), where in part some agglomerations are observed. Crystallization procedure starts at 1000 °C without $Li^+$ doping as testified by Fig. 2(c) and grow into sphere-like particles with average size of 1–2 μm in Fig. 2(d). In contrast, the morphologies of $Li^+$ doped $Eu^{3+}$:$CaWO_4$ are remarkably improved with a clear

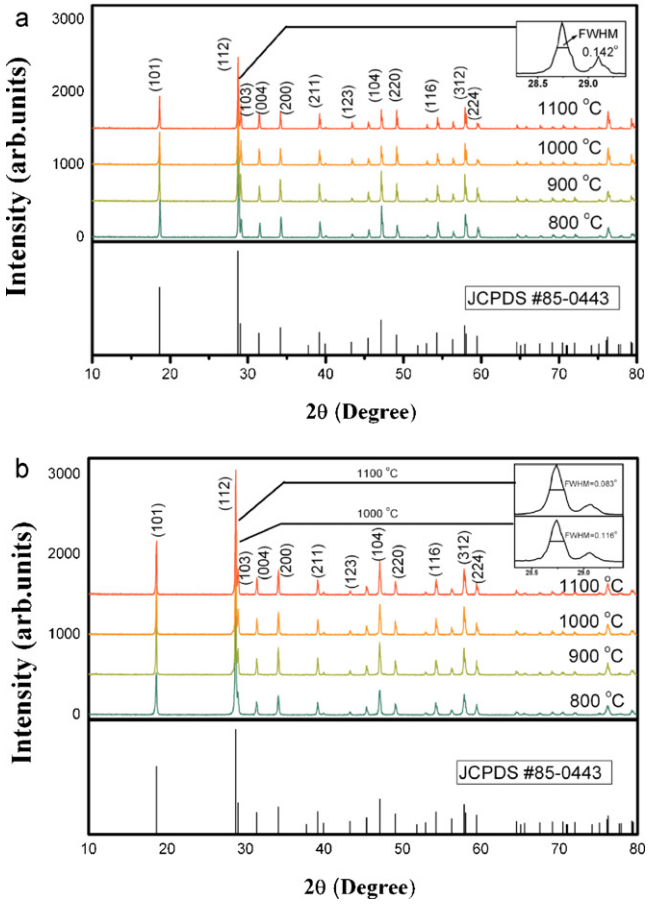


**Fig. 1.** XRD patterns of (a) 10 mol% $Eu^{3+}$ doped $CaWO_4$ and (b) 10 mol% $Eu^{3+}$ and 10 mol% $Li^+$ co-doped $CaWO_4$ prepared at 800–1100 °C and JCPDS Card No. 85-0443 $CaWO_4$. The insets are the enlargement of the (1 1 2) reflection peak of each phosphor sintering at 1000 and 1100 °C, showing significantly reduced fwhm after Li doping.

observation of surface and crystalline boundary after $Li^+$ doping, as shown in Fig. 2(e)–(h). It can be observed that $Ca_{0.8}Eu_{0.1}Li_{0.1}WO_4$ sintered at 800 °C is well crystallized after $Li^+$ doping, the particle size is larger than that of $Ca_{0.9}Eu_{0.1}WO_4$, exhibiting a sphere-like 1–2 μm particles in Fig. 2(e). The Li dopant incorporated into $CaWO_4$ lattice and served as a self-promoter for crystallization and activation is proved even at low temperature of 800 °C. The particles continue to grow into a square shape and consequently forming a uniform distributed crystallization with particle size around 2–3 μm, as shown in Fig. 2(f) and (g). With the increasing of temperature to 1100 °C, aggregation and non-uniform distribution of particles are observed in Fig. 2(h), which is due to the $Li^+$-doping effect comparing to the non-doped one. The assist of grain growth at a low sintering temperature is contributed to the introduction of $Li^+$ component, which is also responsible for the improvement of crystallinity and morphology and consequently with a promotion of PL emission intensity as follows.

### 3.3. XPS analysis

The surface chemical composition of $Li^+$ and $Eu^{3+}$ co-doped $CaWO_4$ phosphors have been characterized by XPS to detect any trace of impurities in the samples as shown in Fig. 3. The carbon species adsorbed on the surface have appeared from the calibration for XPS instrument. Binding energies were calibrated with respect to the signal for adventitious carbon with binding energy of 284.6 eV (1s). The respective binding energies of Ca (2p, 347.2 eV), W (4f, 34.9 eV), O (1s, 530.25 eV), Eu (3d, 1140 eV), and Li (1s,

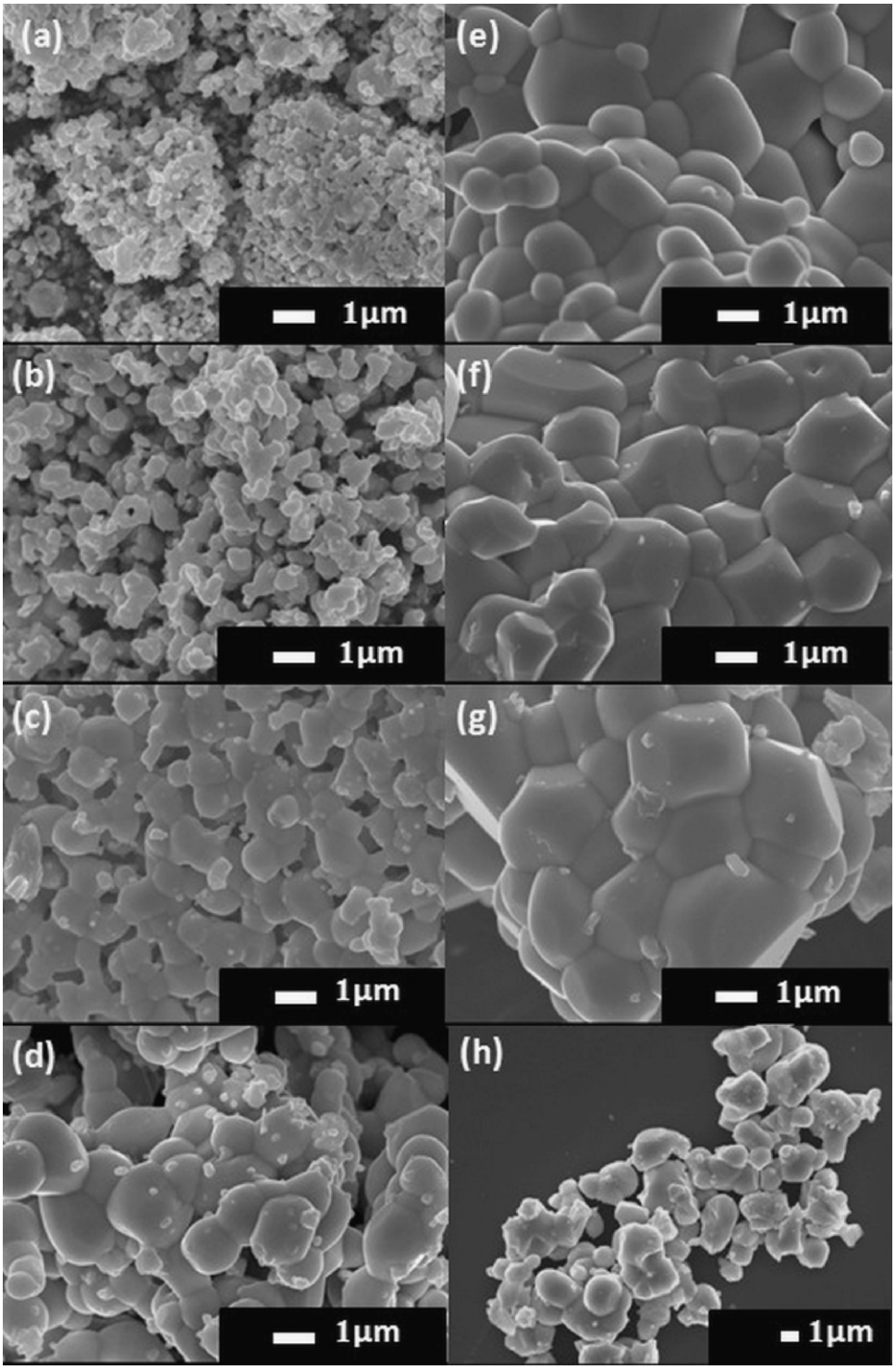


**Fig. 2.** FE-SEM micrographs of 10 mol% of $Eu^{3+}$ doped $CaWO_4$ phosphors sintered at (a) 800, (b) 900, (c) 1000 and (d) 1100 °C, and 10 mol% of $Eu^{3+}$ and 10 mol% $Li^{+}$ co-doped $CaWO_4$ phosphors sintered at (e) 800, (f) 900, (g) 1000, (h) 1100 °C.

50.2 eV) have been observed and also by XRD analysis confirms that no other metal ions can be detected.

### 3.4. Photoluminescence properties

Room-temperature photoluminescence (PL) excitation and emission (PLE) spectra of (a) the $Ca_{0.9}Eu_{0.1}WO_4$ and (b) the $Ca_{0.8}Eu_{0.1}Li_{0.1}WO_4$ sintered at 800–1100 °C are shown in Fig. 4. In the excitation spectrum of $Ca_{0.9}Eu_{0.1}WO_4$, the broad band centered at 270 nm can be ascribed to the charge transfer band (CTB) between $Eu^{3+}$ and $O^{2-}$ ions. Successful doping with $Eu^{3+}$ can be testified by the splitting and intensity patterns of a group of emission lines. The emission spectrum consists of a group of typical $Eu^{3+}$ emission lines, which are mainly located in the spectral area from 550 to 720 nm (in Fig. 4a). These sharp lines are assigned to the $Eu^{3+}$ f–f transitions, where the $Eu^{3+}$ concentration dependence of emission intensity of four characteristic peaks centered at 593, 617, 657 and 704 nm are ascribed to the $^5D_0$–$^7F_J$ ($J$ = 0,

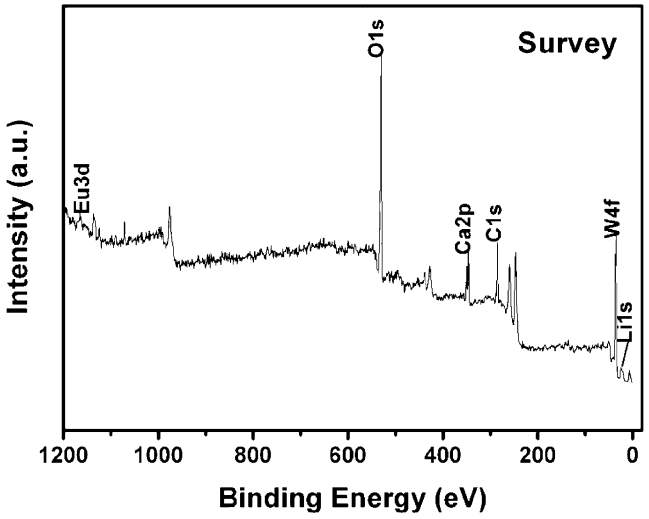


**Fig. 3.** XPS spectra of $Ca_{0.8}Eu_{0.1}Li_{0.1}WO_4$ particles synthesized at 1000 °C.

1, 2, 3, 4) levels of the $Eu^{3+}$ under excitation at 396 nm, respectively. Among these peaks, the dominant electric dipole $^5D_0$–$^7F_2$ transition is hypersensitive, and the emission intensity is strongly affected by the symmetry of host lattice. When the $Eu^{3+}$ occupies a site of non-inversion symmetry, the electric dipole $^5D_0$–$^7F_2$ transition dominates while the magnetic dipole $^5D_0$–$^7F_1$ transition corresponds to a site of inversive centrosymmetry, according to the Judd-Ofelt theory [21].

With the increasing of the temperature, the photoluminescence intensity is accordingly enhanced. Similar results can also be observed in the PL and PLE spectra of $Ca_{0.8}Eu_{0.1}Li_{0.1}WO_4$ in Fig. 4b. This is ascribed to the increasing of the crystalline size upon the raising temperature, which give rise to a decreasing of light scattering [22]. The typical intra-4f transitions of the $Eu^{3+}$ in the excitation spectra and the $^5D_0$–$^7F_J$ ($J$ = 0, 1, 2, 3, 4) transitions of the $Eu^{3+}$ emission spectra are almost the same with that of the $Eu^{3+}$ doped $CaWO_4$. Nevertheless, an obvious shift of CTB toward longer wavelength is observed after $Li^+$ doping. The shift of the CTB toward longer wavelength makes the Li-doped phosphors more efficient for UV absorption. The observed red-shift of the CTB can be attributed to increase of covalence and increase of Eu–O bond length with Li-doping due to weakening of bond strength [23]. As we can see, the intensity of the CTB centered at 297 nm is greatly enhanced. And as well, the emission intensity of the $Ca_{0.8}Eu_{0.1}Li_{0.1}WO_4$ phosphor synthesized at 900 °C is remarkably enhanced after $Li^+$ doping by a factor of 2.8 to that of the $CaWO_4$:$Eu^{3+}$ prepared at 1100 °C, and this value turned out to be 3.0 as the temperature continually increased to 1100 °C, as shown in Fig. 4c. From which we comprehended that with the assistant of $Li^+$ doping, the processing temperature can be decreased as low as 900 °C with a still considerable brightness and it will be beneficial in commercial use.

It is well known that the introduction of $Li^+$ as dopant, even in very small quantities, serves an important role in strengthening of luminescent efficiency of phosphors [24,25]. The concentration dependence of relative PL intensity of $Ca_{1-x}Eu_xWO_4$ and $Ca_{1-2x}Eu_xLi_xWO_4$ ($x$ = 0.02–0.20 mol) under 396 nm excitation was demonstrated in Fig. 5. The intensity of $Eu^{3+}$ emission at 617 nm increased with an increasing doped $Eu^{3+}$ concentration, and then decreased when the concentration exceeding 8 mol% in $Ca_{1-x}Eu_xWO_4$. In comparison with $Ca_{1-x}Eu_xWO_4$, no concentration quenching is observed in the $Ca_{1-2x}Eu_xLi_xWO_4$ phosphors till $x$ = 0.15 mol. As shown in the inset of each figures, the relative intensities is significantly enhanced by a factor of 2.9 in

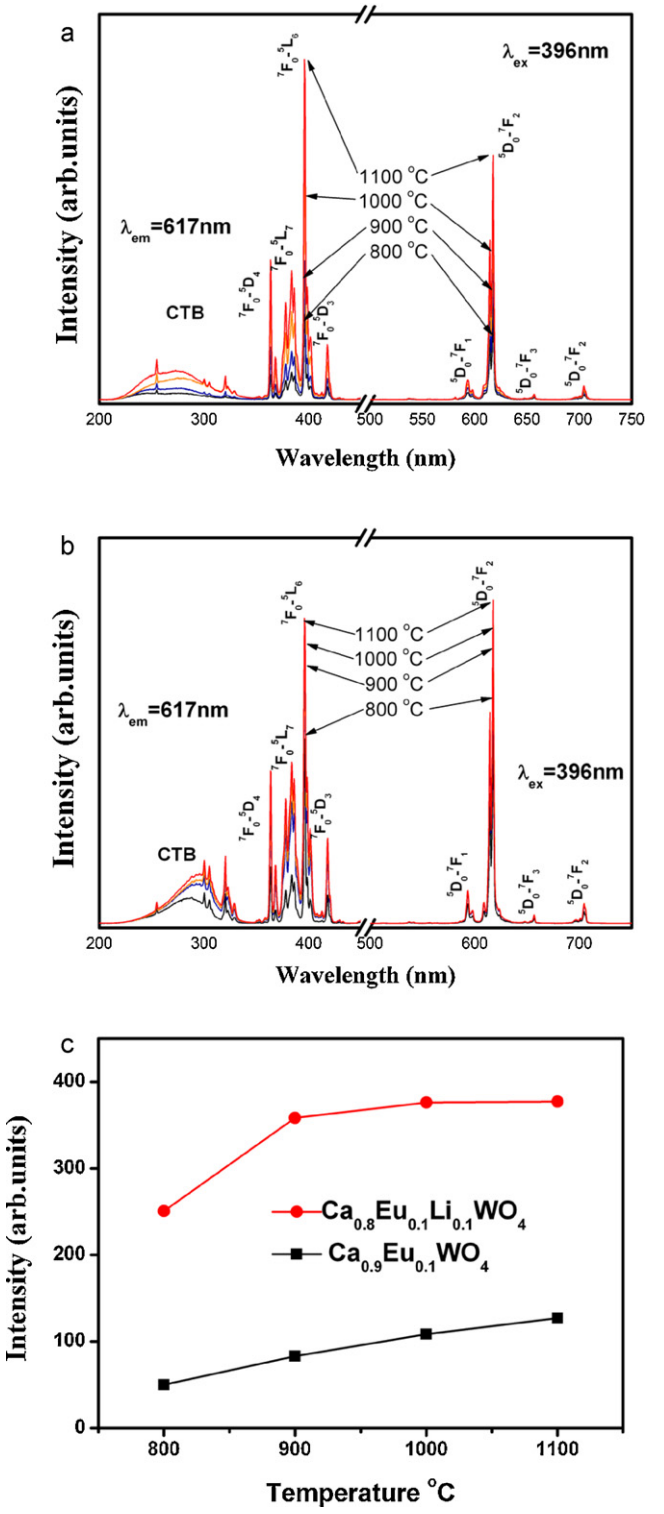


**Fig. 4.** Excitation and emission spectrum of (a) $Ca_{0.9}Eu_{0.1}WO_4$ and (b) $Ca_{0.8}Eu_{0.1}Li_{0.1}WO_4$ phosphors synthesized at 800–1100 °C, and (c) a comparison of relative intensities of $Ca_{0.9}Eu_{0.1}WO_4$ and $Ca_{0.8}Eu_{0.1}Li_{0.1}WO_4$ phosphors.

$Ca_{0.8}Eu_{0.1}Li_{0.1}WO_4$ compare to $Ca_{0.9}Eu_{0.1}WO_4$ phosphors. It is discovered that the incorporation of $Li^+$ into the $CaWO_4$:$Eu^{3+}$ phosphor exhibits not only an enhancement in brightness, but also a diminution of the concentration quenching effect. The sharp lines located from 550 to 720 nm are corresponding to the excited $^5D_0$–$^7F_J$ ($J$ = 0, 1, 2, 3, 4) levels of the f-configuration of $Eu^{3+}$ ion. Amount them, the red emission lines around 617 nm (in Fig. 5) originating from

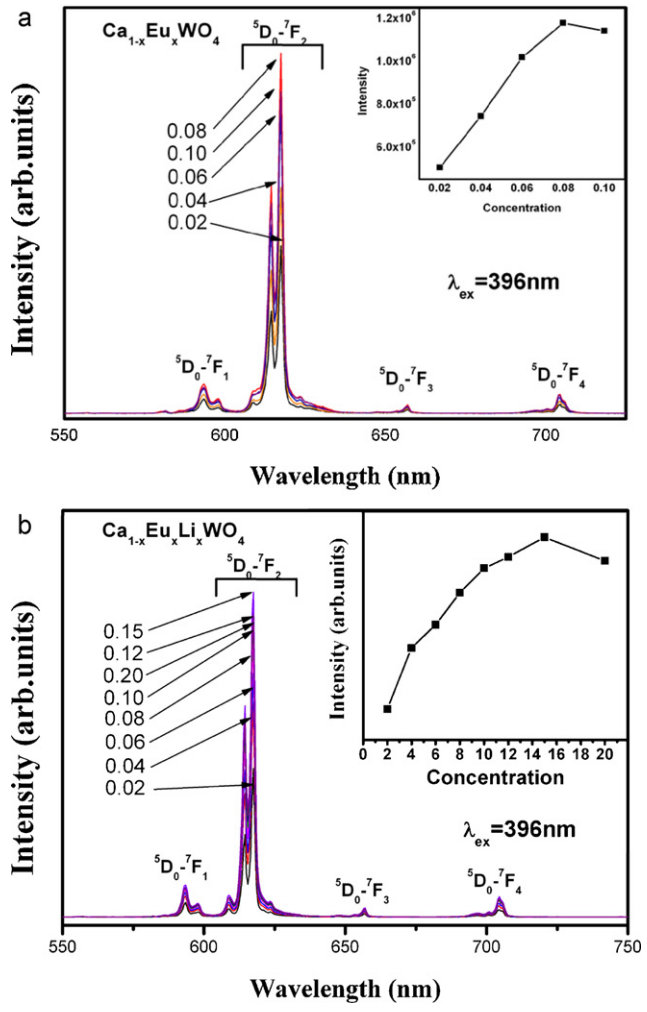


**Fig. 5.** Dependence of PL spectrum of (a) $Ca_{1-x}Eu_xWO_4$ and (b) $Ca_{1-2x}Eu_xLi_xWO_4$ ($x = 0.02 - 0.20$ mol) on $x$, and the inset shows the relative PL intensity as a function of $x$ at $\lambda_{ex} = 396$ nm.

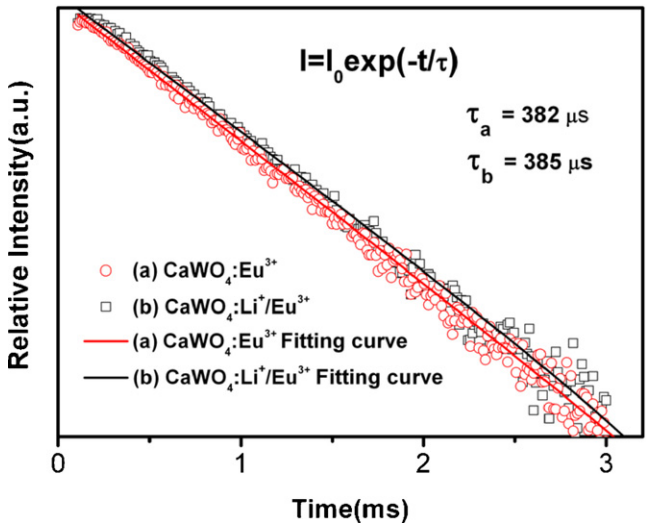


**Fig. 6.** Decay curves of the $^5D_0$–$^7F_2$ transition for the $Ca_{0.1}Eu_{0.9}WO_4$ and $Ca_{0.8}Eu_{0.1}Li_{0.1}WO_4$ phosphors with 396 nm excitation.

electric dipole transition $^5D_0$–$^7F_2$ were the dominant emission for the $Ca_{1-x}Eu_xWO_4$ phosphors, revealing there is no inversion center in this $Eu^{3+}$ doped scheelite-structure. Resultingly, the mechanism of Li dopant was inspected.

When a divalent metallic ion is replaced by a trivalent metallic ion, it is necessary to keep charge balance caused by different valence state. The host has to bringing in $O_2$ from air to solve this problem, and as well brings in defects, which will probably result in the decrease of luminescent properties. In $Ca_{1-2x}Eu_xLi_xWO_4$ phosphor, one $Eu^{3+}$ is expected to substitute one $Ca^{2+}$ ion, thus bring up to a calcium vacancy ($V''_{Ca}$), $3Ca_{Ca} \rightarrow 2Eu_{Ca} + V''_{Ca}$. However, the incorporation of $Li^+$ into host twins the $V''_{Ca}$ and makes a Schottky pair for charge compensation: $2V''_{Ca} + Eu^{3+} + Li^+ \rightarrow Eu_{Ca} + Li'_{Ca}$. With the elimination of defects in the host, $Li^+$ acting as charge compensator is responsible for the enhancement of luminescent properties even at high concentration of 15 mol% of $Eu^{3+}$ ions.

A few transitions that sensitive to the crystal-structure and chemical surroundings are known to be hypersensitive transitions. The electric dipole transition $^5D_0$–$^7F_2$ of $Eu^{3+}$ is hypersensitive transition which can be strongly affected by the ligand ions in the crystal structure. When the $Eu^{3+}$ is located at a low symmetry site, the $^5D_0$–$^7F_2$ often plays the dominant role in the spectrum [26]. The luminescence intensity ratio of $^5D_0$–$^7F_2$ to $^5D_0$–$^7F_1$ reveals the distortion grade from the inversion symmetry of the local environment in the vicinity of $Eu^{3+}$ in the host matrix. Hereby, the intensities of the ED and MD are defined as the area under their PL curves calculated by investigating from 606 to 640 and from 580 to 605 nm, respectively. The symmetry ratio $R = (^5D_0$–$^7F_2)/(^5D_0$–$^7F_1)$ of the $Ca_{1-x}Eu_xWO_4$ and $Ca_{1-2x}Eu_xLi_xWO_4$ with varying $Li^+$ and $Eu^{3+}$ concentration are calculated and listed in Table 1. The asymmetry ratio is independent of Eu or (and) Li concentrations, with the value of around 10.8 in $Ca_{1-x}Eu_xWO_4$ decreasing to 9.4 in average after $Li^+$ doping. The calcium vacancy ($V''_{Ca}$) caused by the substitution of $Eu^{3+}$ for a $Ca^{2+}$ may bring up to a departure of symmetry center on that position, which is eliminated after adding of Li component by reducing the defects, inducing a slight decrease of local symmetry, and furthermore, giving rise to a enhancement of luminescent properties.

Following the National Television System Committee (NTSC) system standard chromaticity, the Commission Internationale de L'Eclairage (CIE) coordinates are calculated and listed in Table 1. With the $Li^+$ ions were introduced into the lattice, the $(x, y)$ values tend to migrate from (0.678, 0.321) to (0.682, 0.317) in average. At the same time, the chromaticity values are independent on the concentration of either $Eu^{3+}$ or $Li^+$ concentrations. Compared with the NTSC standard CIE chromaticity coordinate values for red (0.67, 0.33), this lack of inversion center in the as synthesized $Ca_{1-x}Eu_xWO_4$ and $Ca_{1-2x}Eu_xLi_xWO_4$ provide a high color purity and brightness red phosphor.

Fig. 6 shows the fitted luminescent decay curves of the $^5D_0$–$^7F_2$ transition for the $Ca_{0.1}Eu_{0.9}WO_4$ and $Ca_{0.8}Eu_{0.1}Li_{0.1}WO_4$

**Table 1**
Symmetry ratio $R = (^5D_0$–$^7F_2)/(^5D_0$–$^7F_1)$ and CIE coordinates of the $Ca_{1-x}Eu_xWO_4$ and $Ca_{1-2x}Eu_xLi_xWO_4$ with varying $Li^+$ and $Eu^{3+}$ concentration.

| $x$ value | | 0.02 | 0.04 | 0.06 | 0.08 | 0.1 | Average |
|---|---|---|---|---|---|---|---|
| $Ca_{1-x}Eu_xWO_4$ | $R$ | 10.641 | 10.8382 | 10.8164 | 10.6476 | 11.0695 | 10.80254 |
| | CIE | 0.677, 0.323 | 0.678, 0.321 | 0.679, 0.320 | 0.678, 0.320 | 0.679, 0.320 | 0.678, 0.321 |
| $Ca_{1-2x}Eu_xLi_xWO_4$ | $R$ | 9.57135 | 9.54026 | 9.24294 | 9.3844 | 9.28224 | 9.404238 |
| | CIE | 0.681, 0.318 | 0.682, 0.317 | 0.682, 0.317 | 0.682, 0.317 | 0.683, 0.317 | 0.682, 0.317 |

phosphors. The curves were fitted by a single exponential equation $I = I_0 \exp(-t/\tau)$, where $\tau$ is the life time, and the $I$ and $I_0$ stand for intensity and initial intensity, respectively. Then the decay lifetime of $Ca_{0.1}Eu_{0.9}WO_4$ and $Ca_{0.8}Eu_{0.1}Li_{0.1}WO_4$ phosphors are obtained to be 382 and 385 μs. Since there was seldom much change in the lifetime dependent on the doping of $Li^+$ ion, it can be infer that $Li^+$ doping have no remarkable influence on the radiative relaxation process.

## 4. Conclusion

The $Ca_{1-x}Eu_xWO_4$ and $Ca_{1-2x}Eu_xLi_xWO_4$ phosphors were successfully synthesized by a solid-state reaction method. $Li^+$ ion doping into the host lattice significantly improved the crystallization of the phosphors and enhanced the photoluminescence. The emission intensity of $Ca_{0.8}Eu_{0.1}Li_{0.1}WO_4$ phosphors was improved by a factor of 3.0 after $Li^+$ incorporation. The phosphor prepared at 900 °C provides considerable emission intensity advantage than the non-doping one, while the optimum processing temperature is 1100 °C. The concentration quenching behavior in $Ca_{1-x}Eu_xWO_4$ phosphors is also eliminated after $Li^+$ doping, and the CIE coordinates are calculated to be (0.682, 0.317), which is close to the NTSC standard value. Due to the high quenching temperature and emission intensity, the $Ca_{1-2x}Eu_xLi_xWO_4$ phosphors would be found a promising application on NUV InGaN chip-based white light-emitting diodes.

## Acknowledgments

This work was supported by the National Research Foundation of Korea (NRF) grant funded by the Korea Government (MEST) (No. 2010-0022540). Program also this work was partially supported by NCRC (National Core Research Center) program through the National Research Foundation of Korea funded by the Ministry of Education, Science and Technology (2010-0001-226).

## References

[1] G. Phaomei, W. Rameshwor Singh,.S. Ningthoujam, J. Lumin. 131 (2011) 1164.
[2] F. Zhang, Y.H. Wang, Y. Wen, D. Wang, Y. Tao, Opt. Mater. 33 (2011) 475.
[3] C.K. Chang, T.M. Chen, Appl. Phys. Lett. 90 (2007) 161901.
[4] X.Q. Piao, K.I. Machida, T. Horikawa, H. Hanzawa, Appl. Phys. Lett. 91 (2007) 041908.
[5] S.C. Allen, A.J. Steckl, Appl. Phys. Lett. 92 (2008) 143309.
[6] C.H. Liang, Y.C. Chang, Y.S. Chang, Appl. Phys. Lett. 93 (2008) 211902.
[7] T. Gessmann, E.F. Schubert, J. Appl. Phys. 95 (2004) 2203–2216.
[8] L.Y. Zhou, J.L. Huang, F.Z. Gong, Y.W. Lan, Z.F. Tong, J.H. Sun, J. Alloys Compd. 495 (2010) 268–271.
[9] D. Errandonea, D. Martinez-Garcia, R. Lacomba-Perales, J. Ruiz- Fuertes, A. Segura, Appl. Phys. Lett. 89 (2006) 091913.
[10] M. Minowa, K. Itakura, S. Moriyama, W. Ootani, Nucl. Instrum. Methods Phys. Res. Sect. A 320 (1992) 500.
[11] Z.Y. Zhou, C.X. Li, J. Yang, H.Z. Lian, P.P. Yang, R.T. Chai, Z.Y. Cheng, J. Lin, J. Mater. Chem. 19 (2009) 2737.
[12] R.P. Jia, G.X. Zhang, Q.S. Wu, Y.P. Ding, Appl. Phys. Lett. 89 (2006) 043112.
[13] W.F. Yao, J.H. Ye, J. Phys. Chem. B 110 (2006) 11188.
[14] N. Sharma, K.M. Shaju, G.V.S. Rao, B.V.R. Chowdari, Z.L. Dong, T.J. White, Chem. Mater. 16 (2004) 504.
[15] A. Kudo, M. Steinberg, A.J. Bard, A. Campion, M.A. Fox, T.E. Mallouk, S.E. Webber, J.M. White, Catal. Lett. 5 (1990) 61.
[16] A. Brenier, G.H. Jia, C.Y. Tu, J. Phys.: Condens. Matter 16 (2004) 9103.
[17] G.H. Jia, C.Y. Tu, J.F. Li, X.A. Lu, Z.Y. You, Z.J. Zhu, B.C. Wu, J. Appl. Phys. 98 (2005) 093525.
[18] J.S. Bae, T.E. Hong, J.H. Yoon, B.S. Lee, M.S. Won, J.P. Kim, Y.S. Kim, J.H. Jeong, J. Anal. Sci. Technol. 1 (2) (2010) 92–97.
[19] S.H. Byeon, K.G. Ko, J.C. Park, D.K. Kim, Chem. Mater. 14 (2002) 603.
[20] S.M. Yeh, C.S. Su, Mater. Sci. Eng. B 38 (1996) 245.
[21] S. Shionoya, W.M. Yen, Phosphor Handbook, CRC Press, Boca Raton, FL, 1999, pp. 88 and 179.
[22] C.F. Guo, X. Ding, Y. Xu, J. Am. Ceram. Soc. 93 (6) (2010) 1708–1713.
[23] R. Balakrishnaiah, S.S. Yi, K.W. Jang, H.S. Lee, B.K. Moon, J.H. Jeong, Mater. Res. Bull. 46 (2011) 621–626.
[24] H.K. Yang, J.H. Jeong, J. Phys. Chem. C 114 (1) (2010) 226–230.
[25] T. Hatayama, S. Fukumoto, S. Ibuki, Jpn. J. Appl. Phys. 31 (1992) 3383.
[26] Y.C. Cheng, C.H. Liang, S.A. Yan, Y.S. Chang, J. Phys. Chem. C 114 (2010) 3645–3652.